Critical transition in barrier islands' dune ecosystem and the sudden loss of barrier's resilience

Kiran Adhithya Ramakrishnan[1,2], Tobia Rinaldo[1,3], Ignacio Rodriguez-Iturbe[1], Orencio Durán Vinent[1*]

[1]Department of Ocean Engineering, Texas A&M University, College Station, Texas, USA

[2]Now at the University of Florida (*k.ramakrishnan@ufl.edu*)

[3] Now at UC Berkeley (*t_rinaldo@berkeley.edu*)

[*] *oduranvinent@tamu.edu*

Critical transition in barrier islands' dune ecosystem and the sudden loss of barrier's resilience

Kiran Adhithya Ramakrishnan[1,2+], Tobia Rinaldo[1,3+], Ignacio Rodriguez-Iturbe[1], Orencio Durán Vinent[1*]

[1]*Department of Ocean Engineering, Texas A&M University, College Station, Texas 77843-3136, USA*

[+]*These authors contributed equally to this work*

[2]*Now at the University of Florida (k.ramakrishnan@ufl.edu)*

[3]*Now at UC Berkeley (t_rinaldo@berkeley.edu)*

[*]*oduranvinent@tamu.edu*

Barrier islands cover a large fraction of US coasts and support unique ecosystems and coastal infrastructure. The 'barrier' function of a barrier island depends on coastal dunes that can prevent storm flooding and widespread ecosystem loss. Furthermore, dune-less barriers are more susceptible to breaching and potential drowning under sea level rise. Here we study the transition from richly-vegetated barriers with mature dunes ('high' state) to dune-less barren barriers ('barren' state) using data from a representative set of barrier islands in Virginia, US. We find that these two states are possible stable solutions of a non-linear stochastic dynamics characterized by a tipping point at which barriers with elevation around beach berms experience a critical transition into a permanently barren state. Our results suggest that frequently-flooded dune-less barren islands are a natural endpoint of barrier's evolution under sea level rise (SLR).

Introduction

Barrier islands are dynamic coastal landforms that provide protection from storms and high-energy waves to coastal infrastructure and ecosystems such as marshes, mangroves, oyster reefs and seagrass meadows.

This role is mainly controlled by barrier's elevation and is thus a natural result of the competition between wind-driven sand accretion, which leads to dune formation and increases barrier's elevation, and water-driven (mainly wave runup) dune overtopping that erodes the dunes and decreases barrier's elevation [1–3]. The dunes that represent the highest natural feature on a barrier are the primary structure that dictates the effect of erosional processes on the island by mitigating the impact and reducing the frequency of storm overwashes [4–6]. Without dunes, a barrier island is susceptible to frequent coastal flooding [7], which are expected to accelerate even faster than the global mean sea level rise in the near future [8], and can become barren and potentially drown if sediment supply is low enough [9,10]. A barren barrier, in addition to the expected reduction of biodiversity given the lack of dunes and frequent flooding, would offer little protection to inland coastal infrastructure and ecosystems. As important, low-elevation and narrow barriers undergo a faster landward migration, or marine transgression, as more overwash events are able to transport sand from the beach to the backbarrier [7], potentially exposing stored carbon-rich organic deposits from wetlands and coastal lagoons to high-energy waves at the nearshore [11]. Barrier migration can have a large impact on the size and characteristic of the coastal zone [12] and could potentially shift the carbon budget of the entire coastal system from a net carbon sink to a carbon source [13,14]. Barrier elevation thus offers a good description of barrier state, in which case the formation and post-storm recovery of coastal dunes provide a crucial indication of barrier resilience and ulterior dynamical response to external drivers.

Barrier island dynamics is a complex problem that involves the interaction of sediment transport, hydrodynamics and vegetation across a wide range of spatial and temporal scales [15,16]. Simple models generally focus on the average planform dynamics using mass conservation but without resolving dune dynamics [17–22]. More complex process-based models [23–25] can capture the effect of individual storm impacts on barriers and dunes, whereas large-scale models tend to focus on the long-term barrier response to sediment supply, storms and SLR, but again greatly simplifying the dune dynamics and thus failing to capture the actual stochastic response of barrier elevation [26–32]. A common approach in all models is to resolve the barrier migration rate, which is crucial for the ulterior evolution of the barrier system, using a phenomenological estimation of sand fluxes due to storm overwashes [26,27,32]. Since for a given storm the occurrence and intensity of an overwash event is primarily determined by barrier's elevation, a consistent physical description of barrier migration requires resolving dune dynamics first.

The dynamics of barrier island elevation was recently investigated with a stochastic point model that resolved the competition between dune growth and water-driven vertical erosion that determines whether a barrier island has a dune or not at a given alongshore position [33]. The stochastic model has the advantage of analytically describing the phase space of the barrier elevation state, defined by the probability density function (PDF) of barrier elevation, in terms of two control parameters relating quantities that can be measured remotely. These control parameters determine whether barriers are in a 'high-barrier' state with well-developed dunes, a 'barren' state devoid of dunes and a 'mixed' state where dunes take longer to recovery after erosion and thus washovers (i.e. the sand deposited by an overwash) tend to persist for some time [33].

The probability distribution of barrier elevation in the Virginia Barrier Islands (VBI) (Fig. 1, Methods) indeed shows the three types of barrier islands: 'barren' barriers with elevations close to the beach berm (~ 0.5m) and lacking dunes, 'high' barriers with elevations around mature dunes (~ 2m) as in the case of Hog island, and more complex 'mixed' barriers in between (e.g. South Metompkin). Given the external conditions are similar for all these islands, and assuming similar sand availability, this leads to the question of what controls the transition from a 'high' barrier state, with complex dune and back-barrier ecosystems, to a barren state?

Here we answer this question, and analyze its broader implications, by spatially extending the stochastic point model and then quantitatively testing the model predictions using VBI data (Methods).

Stochastic model of coastal dune dynamics at a point. The stochastic model in [33] describes the time evolution of the PDF of barrier elevation at a point (i.e. at a given alongshore position), where the barrier elevation h is defined as the highest elevation along a cross-shore transect on a barrier island. This model combines a deterministic wind-driven dune growth [34] with stochastic erosion driven by high-water events [35].

High-water events (HWEs) are defined by periods when total water levels (including wave runup) continuously exceed a given threshold, and are well represented by a Marked Poisson process with exponentially distributed marks [35]. The stochastic model assumes this probabilistic description, formally validated for HWEs overtopping elevations up to 0.5m above the characteristic beach elevation [35], can be extended to include the relatively low dunes in our study site, which is consistent with data and simulations of the return period of extreme events in Oregon [35,36]. During dune overtopping conditions, when the mark or size of the HWE exceeds the dune crest, the model assumes for simplicity that the dune is completely eroded up to a base elevation h_0, which is thus defined as the maximum elevation after an overwash. Although in reality there can be partial dune erosion, this assumption captures the onset of the so-called 'overwash regime' in field data [37] and makes analytical calculations possible by ignoring the detailed and complex morphodynamics of dune erosion.

The deterministic dune growth model is based on complex process-based simulations [34] that resolved sand transport, wind aerodynamics and its interaction with the topography, vegetation growth and surface change, and that reproduce the shape and dynamics of real dunes [34,38,39]. Physical simulations [34] showed that dunes grow up to a maximum height H, consistent with field data [3,38]. However, this maximum height is not necessarily constant [40], but depends on slowly varying external conditions such as shoreline position [38] and factors affecting the establishment and survival of dune-building vegetation as reflected in vegetation's distance from the shoreline and elevation above water level [39]. After vegetation colonizes the back-beach and starts trapping wind-driven sand from the beach, and assuming no water overtopping, the simulated dune grows to the maximum height H during a characteristic time T_d following an exponential saturation curve of the form $H(1 - \exp(-t/T_d))$ [34] consistent with data at different barrier islands [3,4,38]. The dune formation time T_d characterizes the undisturbed dune growth in the absence of dune's crest erosion.

For simplicity, the stochastic model assumes that the colonization of the washover by 'dune-building' vegetation after an overwash is much faster than dune formation [33]. In that limit, T_d can be written in terms of the maximum dune growth rate G_d as $T_d = (H - h_0)/G_d$ [34]. The dune growth rate G_d is function of the sand supply from the beach to the dune and, although it is treated as a constant in the model as supported by field data [38], it is a complex quantity that depend on the availability of dry sand on the beach [41], wind direction and intensity, and can be affected by dune toe erosion [40].

The change $\mathrm{d}h$ in barrier elevation after a time interval $\mathrm{d}t$ is modeled by the stochastic equation [33],

$$\mathrm{d}h = \left(\frac{H - h}{T_d}\right)\mathrm{d}t - \Delta h(h, t) \tag{1}$$

where $\Delta h > 0$ is the decrease in dune size after a random HWE [33]. Barrier elevation is assumed to be bounded by the maximum dune height H and the base elevation h_0, and the maximum dune growth rate G_d is assumed to be constant over timescales of the order of a year, large enough to integrate daily and seasonal variations in wind regime and sand supply. Dune model's parameters H, h_0 and G_d will be estimated from data.

The steady state solution of Eq. 1 is given by the point PDF $f_\xi(\xi|\lambda_0^+, \overline{S}^+)$, describing the equilibrium distribution of the random variable ξ over a large-enough time interval and at a particular alongshore position (Methods, Eqs. M1 and M2). The normalized barrier elevation ξ is defined as $\xi = (h - h_0)/(H - h_0)$ and the two control parameters λ_0^+ and $\overline{S}^+$ are: the frequency λ_0 of HWEs overtopping the base elevation

h_0 rescaled by the dune formation time T_d, $\lambda_0^+ = \lambda_0 T_d$; and the average size $\overline{S}$ of the overtopping HWEs rescaled by the maximum dune height relative to the base elevation, $\overline{S}^+ = \overline{S}/(H - h_0)$.

The comparison of the point PDF with an empirical distribution using real data requires a large number of observations frequently sampled over time at the same alongshore location, which is exactly the opposite of how most field data is collected, where elevation is measured over large spatial scales roughly once a year. Therefore, the model has to be expanded alongshore (i.e. parallel to the shoreline) to take advantage of most available data.

Alongshore extension of the point model. In the absence of water-driven erosion and under finite sand supply from the beach, we assume that dunes can form everywhere along a barrier island. In a first approximation, we assume that wind and water forcing, as well as sand availability, are identical in the alongshore direction and that the spatial variations are limited to the randomness associated with preexisting morphology (excluding the dunes) and vegetation characteristics. In that case, only the maximum dune height $H(y)$ and base elevation $h_0(y)$ would change spatially with the alongshore position y. By definition, the alongshore variations of the maximum dune height $H(y)$ represent a simplified characterization of the dune morphology on a barrier island, such that a relatively uniform foredune ridge would be described by a narrow distribution of the values $H(y)$ around the mean dune height, whereas a complex landscape with multiple ridges would be described by a wider distribution encompassing the variety of elevations. Similarly, the alongshore variations of the base elevation $h_0(y)$ would describe the alongshore morphology of superimposed washovers or aeolian backbarrier deposits. Although both H and h_0 can change alongshore randomly, we assume they remain relatively constant over timescales of the order of the dune formation time T_d.

The spatial variation of H and h_0 affects the control parameters of the point PDF which now depend on their local values. Although the change in $\overline{S}^+$ just follows its definition, the change in the rescaled frequency $\lambda_0^+ = \lambda_0 T_d$ is more subtle as both λ_0 and T_d depend on H and h_0. Using the exponential distribution of the size S of HWEs [35], the frequency λ_0 of HWEs overtopping the base elevation h_0 can be written as $\lambda_0 = \lambda_r \exp{(-h_0/\overline{S})}$, where λ_r is the frequency of HWEs overtopping a reference beach elevation at which $h_0 = 0$ by definition [35]. The undisturbed dune formation time is given by $T_d = (H - h_0)/G_d$.

Assuming for simplicity that the alongshore variations in H and h_0 are random and can be approximated by a normal distribution $\mathcal{N}$ (in agreement with the data, Fig. 2), the alongshore PDF $f_h(h)$ is obtained by the integration of the steady-state solution f_ξ at a point (Eqs. M1 and M2), conditioned by H and h_0, over all possible values of the parameters:

$$f_h(h) = \int_0^h \mathcal{N}_{h_0}(h_0) \left(\int_h^\infty \mathcal{N}_H(H) f_{h|H,h_0}(h) \mathrm{d}H \right) \mathrm{d}h_0, \tag{2}$$

where the conditional PDF $f_{h|H,h_0}$ is

$$f_{h|H,h_0}(h) = \frac{1}{H - h_0} f_\xi \left(\frac{h - h_0}{H - h_0} \middle| \lambda_0^+, \overline{S}^+ \right), \tag{3}$$

and the barrier elevation $h(y)$ is a random variable now understood as the highest elevation along cross-shore transects at different locations y alongshore a barrier island.

Assuming for simplicity that the local control parameters $\lambda_0^+(H, h_0)$ and $\overline{S}^+(H, h_0)$ can be approximated by their values at the mean maximum height $\overline{H}$ and mean base elevation $\overline{h}_0$,

$$\overline{S}^+ = \overline{S}/(\overline{H} - \overline{h}_0) \tag{4}$$

$$\lambda_0^+ = \lambda_r e^{-\overline{h}_0/\overline{S}} (\overline{H} - \overline{h}_0)/G_d, \tag{5}$$

they become independent of the local variations and recover their meaning as global control parameters of the alongshore distribution f_h, only function of the average properties along a barrier island.

By describing barrier elevation only by the maximum elevation along a cross-shore profile and simplifying vertical erosion to an all or nothing process, the stochastic model given by Eqs. 2 and 3 reduces the complex shape and dynamics of the barrier surface, including dunes', to a minimal physical description. Indeed, the steady state alongshore elevation distribution f_h only depends on the two control parameters (Eqs. 4 and 5), defined over regional or island-based averages, and the alongshore distributions of the maximum dune height and base elevation, $\mathcal{N}_H$ and $\mathcal{N}_{h_0}$ respectively.

Estimation of model parameters. The average size $\overline{S}$ and mean frequency λ_r of HWEs overtopping the reference beach elevation were estimated for the VBI as 0.3m and 18 events/year respectively [35]. Therefore, Eqs. 2–5 require five parameters (G_d, $\overline{h}_0$, $\overline{H}$ and standard deviations σ_{h_0} and σ_H) to evaluate f_h and compare it to the empirical alongshore distributions (Fig. 1).

A fundamental ingredient of the point model [33], supported by an idealized dune building dynamics [34], is that in the absence of dune erosion, dunes at a given alongshore position grow up to the maximum elevation H selected by the external conditions at that location, and there is a single stable equilibrium in the system: $h = H$. In that case, the point PDF can be approximated as a delta function $f_\xi(\xi) \approx \delta(1 - \xi)$ for a single alongshore location, which leads to $f_h(h) \approx \mathcal{N}_H(h)$ once alongshore fluctuations are taken into account (Eqs. 2 and 3). As expected, in the absence of dune erosion the steady state distribution of barrier elevation f_h is just the alongshore distribution of maximum dune elevation $\mathcal{N}_H$ characterizing the alongshore morphology of mature dunes in the barrier.

In the absence of dune growth, either because of lack of aeolian transport, sediment supply or back-beach vegetation [34] or because dune growth is negligible compared to erosion [33], we expect water-driven transport (by waves and currents) to select a single equilibrium elevation of the barrier, the base elevation h_0 (Fig. 2a–c). This water-driven equilibrium is called a beach berm in barren barriers (e.g. Fig. 1c). In that case, the point PDF becomes $f_\xi(\xi) \approx \delta(\xi)$ and thus $f_h(h) \approx \mathcal{N}_{h_0}(h)$. That is, in the absence of dune growth the steady state distribution of barrier elevation f_h becomes the alongshore distribution of the base elevation $\mathcal{N}_{h_0}$ selected by a balance of water-driven erosion and deposition.

Since by definition neither H nor h_0 change over time (at least over timescales of the order of few years), we can estimate the distributions $\mathcal{N}_{h_0}$ and $\mathcal{N}_H$ by focusing on elevations with negligible growth rate in the VBI data (Fig. 2). In particular, we find that the distribution of steady state elevations can indeed be well approximated by a Gaussian distribution (Fig. 2). The estimated parameters are shown in Table 1 (see Methods for further details, including the estimation of the maximum dune growth rate G_d.) Interestingly, our estimated maximum dune growth rates G_d don't change much for such a diverse group of barrier islands, and are roughly in the range $0.2 - 0.4$m/yr, comparable to measurements from barrier islands in Florida and Texas [3,4], and coastal dunes in Oregon [38].

Results and discussion

Predicted steady states of barrier elevation. As discussed in the introduction, whether a barrier island has a dune or not depends on the competition between dune growth, including sand supply from the beach, and vertical water-driven erosion. For a given pair of control parameters (Table 1), the outcome of this competition is predicted by our model in two different but related ways. The first one is by the alongshore elevation distribution function f_h at the steady state. In spite of the model simplicity and the several assumptions and approximations behind the estimation of the model parameters, the predicted PDF obtained by numerical integration of Eqs. 2 and 3, captures the main characteristics of the empirical distributions for the three years analyzed (Fig. 1b and Fig. 3). Crucially, it reproduces the mode of the empirical distributions and therefore the central quality defining barrier's elevation state: whether the mode is closer to the mean base elevation $\overline{h}_0$, thus defining a 'barren' barrier, or closer to the mean maximum dune height $\overline{H}$, thus defining a 'high' barrier. Barrier steady state is thus completely determined by the control parameters λ_0^+ and $\overline{S}^+$ that regulate the relative weight of the two potential modes of the steady-state point PDF f_ξ: a dune-less mode at $h = h_0$ and the dune mode at $h = H$ [33]. The resulting character of the point PDF is then extended to the alongshore distribution f_h.

The second way to describe barrier's elevation state is by using the mean post-storm dune recovery time $\overline{T}_r^+$, rescaled by the dune formation time. This recovery time is defined as the average time spent by the barrier elevation around the low-elevation mode at $\overline{h}_0$ after an overwash (Eq. M3), and can be interpreted as the average duration of a washover before the dune starts to growth (see Methods for the formal definition). By definition, when the rescaled recovery time is much larger than 1, dunes take very long to recover after erosion. In that case, the island is effectively dune-less (e.g. in a 'barren' state) and its alongshore elevation distribution function at the steady state will have a single mode at the average base elevation interpreted as a beach berm (e.g. Fig. 1b for Cedar island). For example, model prediction for Cedar is $\overline{T}_r^+ \sim 30$ (Fig. 4), which after multiplying by the estimated average dune formation time ($T_d \approx 6$ years, Table 1) leads to a dune recovery time ~ 180 years. On the contrary, when the rescaled recovery time is less than 1, dunes do recover after an overwash, in which case the island will evolve towards a 'high' state with mature dunes. In this case, the alongshore elevation PDF at the steady state has a single mode at the average maximum dune height (see Fig. 1b for Hog island). In between, barriers have widely distributed elevations combining mature dunes and washovers. Therefore, the analytical function $\overline{T}_r^+(\lambda_0^+, \overline{S}^+)$ essentially defines the phase space of barrier state (Fig. 4).

Plotting the values of the control parameters estimated for the VBI in the predicted phase space (Fig. 4) clearly shows that the transition to barren barriers in this region is essentially driven by a 30-fold increase in the rescaled frequency of HWEs (λ_0^+). From its definition (Eq. 5), the rescaled frequency is particularly sensitive to the mean base elevation $\overline{h}_0$ (it decreases exponentially with it) compared to other parameters such as the relative maximum dune height ($\overline{H} - \overline{h}_0$) or the maximum dune growth rate (G_d). Indeed, changing only $\overline{h}_0$ while keeping all the other parameters as estimated for Hog creates a phase curve (i.e. a path in the phase space) that describes a potential transition from Hog to South Metompkin and eventually Cedar, Smith and North Metompkin (Fig. 4, dashed line). Therefore, in the VBI, the transition to a barren state seems to be mainly controlled by the mean base elevation of the barriers.

Robustness of model predictions. The most important model prediction is related to the steady state of the barrier island and thus only depends on the control parameters (Eqs. 4 and 5). Parameters such as the standard deviations of the base elevation and the maximum dune height, or even the type of random distribution, certainly affects the shape of the alongshore PDF (Fig. 3) but not the position of the modes that define the barrier state. Interestingly, the transition to a barren state, as described by the rescaled dune recovery time in Fig. 4, depends weakly on the mean maximum dune height $\overline{H}$. This is because, in a first-order approximation at the transition from 'mixed' to 'barren' states, the dune recovery time is only function of the product of the control parameters [33] $\lambda_0^+ \overline{S}^+$ and this product does not depend on $\overline{H}$ (Eqs. 4 and 5). As a result, the uncertainty in our estimations of the maximum dune height, in particular for barren barriers, has little impact in our final results. This extends to model simplifications such as neglecting shoreline change and ignoring vegetation characteristics and dynamics, which mainly affect the size and shape of mature dunes [38,39,42]. Furthermore, by focusing on post-storm dune recovery (which mainly depends on the erosion of proto-dunes [2]) and not on the erosion of mature dunes, our predictions are relatively insensitive to the way we model the probabilistic properties of extreme events, and our simplified description of the degree of dune erosion after overtopping.

Irreversibility of the barren state. VBI data suggest that the transition to a barren state take place at $\overline{h}_0 \approx 0.4$m, that is, when the mean base elevation $\overline{h}_0$ is determined by the beach berm and thus purely controlled by water-driven transport. As shown in Fig. 2(a-c), this barrier elevation ($h \approx 0.4$m) is a relatively strong attractor of the water-driven dynamics as elevations up to twice or more tend to be eroded in average, in agreement with the predicted stochastic model dynamics. Indeed, the barren state is a stable state in the stochastic model precisely because erosion dominates dune formation for barrier elevations around the beach berm. This also suggests the barren state is irreversible as water-driven processes cannot increase the mean base elevation above the beach berm once dunes are eroded following a large storm.

Effect of sea level rise. The model insight into the fundamental role played by the mean base elevation ($\overline{h}_0$) in controlling barrier state allows for a novel way sea level rise (SLR) can impact barrier islands. Since h_0 is defined relative to a reference beach elevation tied to the water level [35], in the absence of sand accretion at a scale larger than the dune width, $\overline{h}_0$ would just decrease with SLR over time until the barrier undergoes a transition to the lower elevation state (Fig. 5). Using the intermediate scenario for the average rate of relative sea level rise (RRSLR) in the study site from 2020-2050 (RRSLR $\approx$ 10mm/yr) [43] it would take ~ 25 years for $\overline{h}_0$ to decrease 0.25m (Fig. 5), which is the difference between the mean base elevation of South Metompkin, a 'high'/'mixed' barrier, and Parramore, a relatively barren barrier (Fig. 4 and Table 1).

More generally, by only decreasing $\overline{h}_0$, SLR effectively increases the rescaled frequency of erosional events (HWEs), decreases the dune recovery time and thus drives a potentially irreversible transition to the 'barren' equilibrium state. As shown in Fig. 5, this shift in barrier equilibrium can take place in a couple of decades, which is almost certainly an underestimation because we are ignoring the expected increase in the frequency of wave-driven coastal flooding [8].

Critical transition in barrier islands' dune ecosystem. The loss of coastal dunes and the transition to a barren state, driven by changes in the rescaled frequency of HWEs (λ_0^+) and exemplified by the phase curve in Fig. 4, is an example of critical transition in a complex stochastic system [44] (Fig. 5). As the mean base elevation of the barrier decreases with SLR, λ_0^+ increases and external fluctuations in HWEs, and the internal randomness in the underlying morphology, force the barrier to explore different elevations at different frequencies. The frequencies are given by $f_h(h|\lambda_0^+(t))$ if changes are slow enough for the system to remain close to the equilibrium state, and can be used to infer the basin of attraction of the two main equilibrium elevations [44] (Fig. 5b-e): the mean base elevation $\overline{h}_0(t)$, itself function of time via SLR, and the mean maximum dune height $\overline{H}$, which is selected by the interaction of the dune-building plant ecosystem and shoreline-related abiotic stressors [34]. As $\overline{h}_0(t)$ approaches the 0.5m threshold suggested by the data ($\lambda_0^+ \approx 20$), the basin of attraction of $\overline{H}$ becomes shallower and the recovery time greatly increases, in what is called a critical slowing down (Fig. 5d). For even lower values of $\overline{h}_0(t)$, the dune basin of attraction essentially dissapears and the barrier crosses a tipping point with its state relaxing towards the 'barren' equilibirum as eroded dunes cannot recover (Fig. 5e). This stochastic picture both formalizes and generalizes a previous interpretation of barrier dynamics as bi-stable [1] which is not a suitable description of a stochastic system.

In this context, the rescaled dune recovery time $\overline{T}_r^+$ [33], interpreted as the average time to escape the low-elevation basin of attraction, provides a metric to evaluate the critical slowing down that characterizes the system close to the tipping point [44] and can thus formally describe barrier's resilience.

Implications for our understanding of barrier dynamics. Barrier islands, and the dune and dune ecosystems on them, are very complex systems integrating water and wind-driven sediment transport to the dynamics of different plant ecosystems under the influence of tides, waves, wind and storms [16]. Here we showed that, in spite of this complexity, barrier elevation can be well described by a relatively simple physics-based stochastic model in terms of a few basic parameters: the frequency and average intensity of high-water events, the dune growth rate, the maximum dune height and the base elevation after an overwash. The last three in particular capture the complexity of the system in different ways. The alongshore distribution of the maximum dune height captures the morphology of mature dunes along with the eco-geomorphic processes controlling it, including type and characteristics of 'dune-building' vegetation and the effects of shoreline change. Similarly, the alongshore distribution of the base elevation captures the outcome of overwashes, beach berm' dynamics and any preexisting morphology. Finally, the island-based maximum dune growth rate contains all the spatiotemporal complexity of sand transport, including sand availability, taking place in the bare surface between the shoreline and any dense vegetation layer. Interestingly, the apparent randomness of the alongshore distribution (over large enough spatial scales) suggests that only the mean values (for both maximum dune height and base elevation) have physical meaning and that minor alongshore variations due to the spatial complexity of the underlying processes can be characterized as random noise. This is in contrast to other approaches attempting to correlate all the details of the alongshore variation of dune and barrier morphology to many potentially relevant parameters acting over relatively small spatial scales [45,46].

We would like to emphasize that the predictions from the stochastic model concern only the steady state of barrier elevation and not barrier's current state. A barrier can be classified as 'barren' based on the estimated control parameters and still have well-developed dunes (or vice versa). However, such barrier would lack resilience since dunes cannot recover after erosion and thus, by the definition, the barrier would remain barren. In this context, the very large return period of the extreme events (e.g. large storms) needed to completely erode meters-tall dunes can prove misleading because the relaxation to the 'barren' equilibrium can be greatly accelerated by shoreline erosion, which can erode dunes at a much faster rate. Shoreline erosion can then 'push' the system into the 'barren' equilibrium made possible by passive inundation under SLR, in which case we would expect more barren barriers in regions with larger erosion rate [47,48]. This mechanism would connect barrier resiliency to the local underlying geology and erosion rates [48,49].

Barrier elevation state is also closely related to its migration rate, as a barrier in a 'high' state would barely migrate, essentially shrinking and sinking under SLR until potentially transitioning into the 'barren' state where it would experience a maximum migration rate function of the underlying geology [50]. In fact, under some approximations, the solution of the stochastic model can be used to estimate the average overwash-driven sand flux across a barrier island [33]. This could improve the predictions of large-scale coastal models that don't resolve the actual dune dynamics and could allow us to better understand the effect of the expected acceleration in barrier migration on the overall barrier system [26,51]. Therefore, although the transition into a 'barren' state doesn't necessarily lead to drowning, because a barrier island lacking dunes can still have a large marsh platform that prevents it to become a submerged shoal (as it's the case with most of the barren islands in the VBI), identifying a change in barrier equilibirum from a 'high' to the 'barren' state could be the very first indication of a broader shift in the global coastal system.

Placing barrier islands in the broader class of (eco)systems undergoing critical transitions [52] has the potential to advance the theoretical understanding of coastal dynamics at different spatial and temporal scales, and lead to simpler large-scale coastal models suitable for inclusion into Earth system models [53] and models coupling human-coastal system to natural and socioeconomic drivers [54,55].

1. Durán Vinent, O. & Moore, L. J. Barrier island bistability induced by biophysical interactions. *Nature Climate Change* **5**, 158–162 (2015).

2. Houser, C. & Hamilton, S. Sensitivity of post-hurricane beach and dune recovery to event frequency. *Earth Surface Processes and Landforms* **628**, 613–628 (2009).

3. Houser, C. *et al.* Post-storm beach and dune recovery: Implications for barrier island resilience. *Geomorphology* **234**, 54–63 (2015).

4. Priestas, A. & Fagherazzi, S. Morphological barrier island changes and recovery of dunes after Hurricane Dennis, St. George Island, Florida. *Geomorphology* **114**, 614–626 (2010).

5. Morton, R. A. & Sallenger Jr, A. H. Morphological impacts of extreme storms on sandy beaches and barriers. *Journal of Coastal Research* 560–573 (2003).

6. Houser, C. *et al.* Role of the foredune in controlling barrier island response to sea level rise. In *Barrier dynamics and response to changing climate*, 175–207 (Springer, 2018).

7. Rodriguez, A. B., Yu, W. & Theuerkauf, E. J. Abrupt Increase in Washover Deposition Along a Transgressive Barrier Island During the Late Nineteenth Century Acceleration in Sea-Level Rise. In Moore, L. J. & Murray, A. B. (eds.) *Barrier Dynamics and Response to Changing Climate*, 121–145 (Springer International Publishing, Cham, 2018).

8. Almar, R. *et al.* A global analysis of extreme coastal water levels with implications for potential coastal overtopping. *Nature Communications* **12**, 3775 (2021).

9. Penland, S., Boyd, R. & Suter, J. R. Transgressive Depositional Systems of the Mississippi Delta Plain: A Model for Barrier Shoreline and Shelf Sand Development. *Journal of Sedimentary Research* **58**, 932–949 (1988).

10. Mellett, C. L. & Plater, A. J. Drowned Barriers as Archives of Coastal-Response to Sea-Level Rise. In Moore, L. J. & Murray, A. B. (eds.) *Barrier Dynamics and Response to Changing Climate*, 57–89 (Springer International Publishing, Cham, 2018).

11. Deaton, C. D., Hein, C. J. & Kirwan, M. L. Barrier island migration dominates ecogeomorphic feedbacks and drives salt marsh loss along the Virginia Atlantic Coast, USA. *Geology* **45**, 123–126 (2017).

12. Hein, C. J. & Kirwan, M. L. Marine Transgression in Modern Times. *Annual Review of Marine Science* **16**, annurev–marine–022123–103802 (2024).

13. Theuerkauf, E. J. & Rodriguez, A. B. Placing barrier-island transgression in a blue-carbon context. *Earth's Future* **5**, 789–810 (2017).

14. Kirwan, M. L., Megonigal, J. P., Noyce, G. L. & Smith, A. J. Geomorphic and ecological constraints on the coastal carbon sink. *Nature Reviews Earth & Environment* **4**, 393–406 (2023).

15. Stallins, J. A. Stability domains in barrier island dune systems. *Ecological Complexity* **2**, 410–430 (2005).

16. Zinnert, J. C., Stallins, J. A., Brantley, S. T. & Young, D. R. Crossing Scales: The Complexity of Barrier-Island Processes for Predicting Future Change. *BioScience* **67**, 39–52 (2017).

17. Wolinsky, M. A. & Murray, A. B. A unifying framework for shoreline migration: 2. application to wave-dominated coasts. *Journal of Geophysical Research: Earth Surface* **114** (2009).

18. Murray, A. B. & Moore, L. J. Geometric constraints on long-term barrier migration: from simple to surprising. In *Barrier dynamics and response to changing climate*, 211–241 (Springer, 2018).

19. Cowell, P., Roy, P. & Jones, R. Simulation of large-scale coastal change using a morphological behaviour model. *Marine Geology* **126**, 45–61 (1995).

20. Stolper, D., List, J. H. & Thieler, E. R. Simulating the evolution of coastal morphology and stratigraphy with a new morphological-behaviour model (geombest). *Marine Geology* **218**, 17–36 (2005).

21. Moore, L. J., List, J. H., Williams, S. J. & Stolper, D. Complexities in barrier island response to sea level rise: Insights from numerical model experiments, north carolina outer banks. *Journal of Geophysical Research: Earth Surface* **115** (2010).

22. Walters, D., Moore, L. J., Duran Vinent, O., Fagherazzi, S. & Mariotti, G. Interactions between barrier islands and backbarrier marshes affect island system response to sea level rise: Insights from a coupled model. *Journal of Geophysical Research: Earth Surface* **119**, 2013–2031 (2014).

23. Roelvink, D. *et al.* Modelling storm impacts on beaches, dunes and barrier islands. *Coastal engineering* **56**, 1133–1152 (2009).

24. McCall, R. T. *et al.* Two-dimensional time dependent hurricane overwash and erosion modeling at santa rosa island. *Coastal Engineering* **57**, 668–683 (2010).

25. Harter, C. & Figlus, J. Numerical modeling of the morphodynamic response of a low-lying barrier island beach and foredune system inundated during hurricane ike using xbeach and cshore. *Coastal Engineering* **120**, 64–74 (2017).

26. Mariotti, G. & Hein, C. J. Lag in response of coastal barrier-island retreat to sea-level rise. *Nature Geoscience* **15**, 633–638 (2022).

27. Reeves, I., Moore, L., Murray, A., Anarde, K. & Goldstein, E. Dune dynamics drive discontinuous barrier retreat. *Geophysical Research Letters* **48**, e2021GL092958 (2021).

28. Nienhuis, J. H. & Lorenzo-Trueba, J. Simulating barrier island response to sea level rise with the barrier island and inlet environment (brie) model v1. 0. *Geoscientific Model Development* **12**, 4013–4030 (2019).

29. Lorenzo-Trueba, J. & Ashton, A. D. Rollover, drowning, and discontinuous retreat: Distinct modes of barrier response to sea-level rise arising from a simple morphodynamic model. *Journal of Geophysical Research: Earth Surface* **119**, 779–801 (2014).

30. Storms, J. E., Weltje, G. J., Van Dijke, J., Geel, C. & Kroonenberg, S. Process-response modeling of wave-dominated coastal systems: simulating evolution and stratigraphy on geological timescales. *Journal of sedimentary Research* **72**, 226–239 (2002).

31. Rosati, J. D., Dean, R. G. & Stone, G. W. A cross-shore model of barrier island migration over a compressible substrate. *Marine Geology* **271**, 1–16 (2010).

32. Bamunawala, J., van der Spek, A., Dastgheib, A., Murray, A. B. & Ranasinghe, R. An Integrated, Probabilistic Modeling Approach to Assess the Evolution of Barrier-Island Systems Over the Twenty-First Century. *Frontiers in Marine Science* **8** (2021).

33. Vinent, O. D., Schaffer, B. E. & Rodriguez-Iturbe, I. Stochastic dynamics of barrier island elevation. *Proceedings of the National Academy of Sciences* **118** (2021).

34. Durán, O. & Moore, L. J. Vegetation controls on the maximum size of coastal dunes. *Proceedings of the National Academy of Sciences of the United States of America* **110**, 17217–22 (2013).

35. Rinaldo, T., Ramakrishnan, K. A., Rodriguez-Iturbe, I. & Vinent, O. D. Probabilistic structure of events controlling the after-storm recovery of coastal dunes. *Proceedings of the National Academy of Sciences* **118** (2021).

36. Serafin, K. A. & Ruggiero, P. Simulating extreme total water levels using a time-dependent, extreme value approach. *Journal of Geophysical Research: Oceans* **119**, 6305–6329 (2014).

37. Long, J. W., de Bakker, A. T. M. & Plant, N. G. Scaling coastal dune elevation changes across storm-impact regimes. *Geophysical Research Letters* **41**, 2899–2906 (2014).

38. Moore, L. J., Vinent, O. D. & Ruggiero, P. Vegetation control allows autocyclic formation of multiple dunes on prograding coasts. *Geology* **44**, 559–562 (2016).

39. Hovenga, P. A. *et al.* Quantifying the relative influence of coastal foredune growth factors on the U.S. Mid-Atlantic Coast using field observations and the process-based numerical model Windsurf. *Coastal Engineering* **181**, 104272 (2023).

40. Davidson-Arnott, R. *et al.* Sediment budget controls on foredune height: Comparing simulation model results with field data. *Earth Surface Processes and Landforms* **43**, 1798–1810 (2018).

41. Houser, C. Synchronization of transport and supply in beach-dune interaction. *Progress in Physical Geography* **33**, 733–746 (2009).

42. Ruggiero, P., Hacker, S., Seabloom, E. & Zarnetske, P. The role of vegetation in determining dune morphology, exposure to sea-level rise, and storm-induced coastal hazards: a us pacific northwest perspective. In *Barrier dynamics and response to changing climate*, 337–361 (Springer, 2018).

43. Sweet, W. *et al.* Global and regional sea level rise scenarios for the united states: Updated mean projections and extreme water level probabilities along u.s. coastlines. Tech. Rep., NOAA Technical Report NOS 01. National Oceanic and Atmospheric Administration. National Ocean Service, Silver Spring, MD (2022).

44. Scheffer, M. *et al.* Anticipating Critical Transitions. *Science* **338**, 344–348 (2012).

45. Jay, K. R., Hacker, S. D., Hovenga, P. A., Moore, L. J. & Ruggiero, P. Sand supply and dune grass species density affect foredune shape along the US Central Atlantic Coast. *Ecosphere* **13**, e4256 (2022).

46. Gutierrez, B. T., Plant, N. G., Thieler, E. R. & Turecek, A. Using a Bayesian network to predict barrier island geomorphologic characteristics. *Journal of Geophysical Research: Earth Surface* **120**, 2452–2475 (2015).

47. Morton, R. A. & Miller, T. L. National assessment of shoreline change: Part 2: Historical shoreline changes and associated coastal land loss along the U.S. Southeast Atlantic Coas. Open-File Report 2005-1401, U.S. Geological Survey (2005).

48. Twichell, D. C., Flocks, J. G., Pendleton, E. A. & Baldwin, W. E. Geologic Controls on Regional and Local Erosion Rates of Three Northern Gulf of Mexico Barrier-Island Systems. *Journal of Coastal Research* **63**, 32–45 (2013).

49. Wernette, P. *et al.* Influence of a spatially complex framework geology on barrier island geomorphology. *Marine Geology* **398**, 151–162 (2018).

50. Murray, A. B. & Moore, L. J. Geometric Constraints on Long-Term Barrier Migration: From Simple to Surprising. In Moore, L. J. & Murray, A. B. (eds.) *Barrier Dynamics and Response to Changing Climate*, 211–241 (Springer International Publishing, Cham, 2018).

51. Moore, L. J. & Murray, A. B. Islands on the move. *Nature Geoscience* **15**, 602–603 (2022).

52. Lever, J. J. *et al.* Foreseeing the future of mutualistic communities beyond collapse. *Ecology Letters* **23**, 2–15 (2020).

53. Ward, N. D. *et al.* Representing the function and sensitivity of coastal interfaces in Earth system models. *Nature Communications* **11**, 2458 (2020).

54. Kopp, R. E. *et al.* Usable Science for Managing the Risks of Sea-Level Rise. *Earth's Future* **7**, 1235–1269 (2019).

55. McNamara, D. E., Lazarus, E. D. & Goldstein, E. B. Human–coastal coupled systems: Ten questions. *Cambridge Prisms: Coastal Futures* **1**, e20 (2023).

56. Wernette, P., Houser, C. & Bishop, M. P. An automated approach for extracting barrier island morphology from digital elevation models. *Geomorphology* **262**, 1–7 (2016).

METHODS

Extraction of alongshore barrier elevation data. Digital elevation models (DEM) of the Virginia barrier islands for three different years (2014, 2016, 2017) were obtained from the USGS Lidar scans (`www.ncei.noaa.gov/maps/bathymetry/`). The data, originally referred to the NAVD88 datum, was shifted relative to a representative value of the beach elevation, 1.5m, obtained from the analysis of high water event (HWEs) and related to the average wave run-up [35]. We use this reference beach elevation as an unbiased way to define the body of the islands that naturally excludes the back-barrier marshes and other low-elevation features unrelated to wave-driven transport (Fig. S2). Homogeneous parts of each island were considered to ensure a stationary process with the help of features present in the DEM, for e.g. Metompkin island was split into two portions since the southern portion of the island presents a partial dune system whereas the northern portion lacks any dunes. Islands where shrubs were exposed to the shoreline due to coastal erosion were not considered for the analysis. Cross-shore lines were constructed on natural portions of the selected barrier islands at a constant spacing of 10m using GIS software. For each cross-shore line (alongshore position y) and year (t), the barrier elevation $h(y,t)$ was extracted as the maximum elevation along the cross-shore profile. Therefore, the alongshore elevation profile $h(y,t)$ includes all possible features in the barrier island: beach berms, overwash fans, primary dunes (or foredunes) and secondary dunes. For narrow islands (i.e. islands without secondary dunes) this method extracts the dune height without the complexity involved in the precise determination of the foredune crest [56]. By definition a positive elevation ($h(y) > 0$) means the feature at y is above the reference beach elevation.

Steady-state point PDF. From the stochastic point model in [33], the steady-state PDF of the rescaled barrier elevation ξ is

$$f_\xi(\xi) = \left(\int_0^1 \frac{\phi(\xi)}{1-\xi} \, d\xi \right)^{-1} \frac{\phi(\xi)}{1-\xi} \tag{M1}$$

where

$$\phi(\xi) = \exp\left[-\lambda_0^+ e^{-\frac{1}{\overline{S}^+}} \left(E_i\left(\frac{1}{\overline{S}^+}\right) - E_i\left(\frac{1-\xi}{\overline{S}^+}\right)\right)\right]. \tag{M2}$$

and the exponential integral is $E_i(x) = -\int_{-x}^{\infty} x^{-1}e^{-x}\mathrm{d}x$.

The PDF $f_\xi(\xi)$ has a minimum at $\xi_{\min} = \overline{S}^+ \ln \lambda_0^+$ and therefore is strictly bimodal for $0 < \xi_{\min} < 1$.

Mean dune recovery time. The rescaled mean dune recovery time $\overline{T}_r^+$ is defined as the mean excursion time below the minimum of the steady state ($\xi_{\min}$) divided by the dune formation time T_d. From [33]

$$\overline{T}_r^+ = \frac{1}{\phi(\xi_{\min})} \int_0^{\xi_{\min}} \frac{\phi(\xi')}{1-\xi'} \mathrm{d}\xi' . \tag{M3}$$

Outside the bimodal region, $\overline{T}_r \equiv 0$ when f_ξ has a single high-elevation mode ($\xi_{\min} \leq 0$ for $\lambda_0^+ \leq 1$), and $\overline{T}_r \to \infty$ when f_ξ has a single low-elevation mode ($\xi_{\min} \geq 1$ for $\lambda_0^+ \geq e^{1/\overline{S}^+}$, white region in Fig. 4).

Estimation of model parameters: base elevation. At the steady state we expect the PDF f_s of stable elevations to be approximated as $f_s(h) = a_0\mathcal{N}_{h_0}(h) + (1-a_0)\mathcal{N}_N(h)$ with normalization constant a_0. This constant depends on the relative contribution of dune growth and erosion in the resulting stochastic dynamics, such that $a_0 \sim 0$ when erosional processes dominate whereas $a_0 \sim 1$ otherwise. However, the complexity of barrier island dynamics and the fact that elevation data for the rate calculation is three years apart, and therefore we are sampling over several realizations of the stochastic process, imply that deviations from the ideal form of f_s are to be expected (Fig. 2 and Fig. S1).

In spite of the inherent uncertainty of this method, fitting f_s by two Gaussians seems to capture the distribution $\mathcal{N}_{h_0}$ of base elevations, and thus $\overline{h}_0$ and σ_{h_0}, relatively well (solid red lines in Fig. 2 and Fig. S1). Indeed, for the ‘barren’ barriers (Cedar, North Metompkin and Smith) the corresponding mean base elevation $\overline{h}_0$ reproduces the lower (beach berm) equilibrium of barrier elevation, defined by the conditions $G = 0$ and $G' < 0$ on the average growth rate function $G(h)$ (red dots in Fig. 2a and Fig. S1 a,b), and the growth rate can be well approximated by the linear function $G(h) = (\overline{h}_0 - h)/\Delta t$, with $\Delta t = 3$yr (black dashed lines in Fig. 2a and Fig. S1 a,b).

In Hog and Parramore, $\overline{h}_0$ corresponds to a local minimum of $G(h)$ (red dots in Fig. 2b and Fig. S1c), similar to South Metompkin (Fig. S1d).

The larger standard deviation for South Metompkin (Table 1) is due to the presence of several overwash fans with a relatively complex morphology as compared with the more uniform beach berm morphology in 'barren' barriers (Figs. S2).

Estimation of model parameters: maximum dune height. The extraction of the distribution of maximum dune elevations $\mathcal{N}_H$ is more challenging as not all barriers have well-developed dunes. For Hog and South Metompkin, f_s peaks at elevations $\sim$ 2m and can be used to estimate $\mathcal{N}_H$, and thus $\overline{H}$ and σ_H (blue lines in Fig. 2 k and l). The other islands don't have a well-developed dune system and therefore the fitted higher elevation Gaussian (gray lines in Fig. 2 g, i and j) cannot be used to properly estimate $\mathcal{N}_H$. Interestingly, the value $\overline{H} \sim 2$m from Hog is consistent with the dune stable equilibrium in Smith (blue dot in Fig. 2 c), defined by the conditions $G = 0$ and $G' < 0$ on the average growth rate function $G(h)$ (solid black line in Fig. 2 c).

In general, for islands other than Hog or South Metompkin, $\overline{H}$ and σ_H are approximated by their values for Hog, which is assumed to be representative of a well-developed dune system in the region. For Parramore, we assume $\overline{H}$ can be approximated by the dune equilibrium elevation (blue dot in Fig. 2 d) and use the standard deviation of the fitted higher elevation Gaussian (gray line in Fig. 2 j) as an approximation for σ_H.

Note that the larger standard deviation for South Metompkin (Table 1) reflects a complex morphology with primary and secondary relic dunes (Fig. S1), which are included in the way we define the barrier elevation data. In contrast, the relatively narrow distribution in Hog reflects its single, and relatively uniform, dune ridge (Fig. S1).

Estimation of model parameters: maximum dune growth rate. We estimate the maximum dune growth rate G_d as the average of the ten highest growth rates (excluding the maximum) for initial elevations above the typical beach berm (approximated here as 0.4m) where the potential availability of dry sand and presence of vegetation allows dune building (red dashed lines in Fig. 2a-f).

Data availability The data generated by this study will be made available before publication.

Code availability The code that integrates the equations can be made available upon request to the authors.

Acknowledgments TR, IRI and ODV acknowledge the support of the Texas A&M Engineering Experiment Station (TEES). KAR acknowledge the support of a fellowship from the Hagler Institute at Texas A&M University.

Author contributions ODV and IRI designed the research; KAR and TR generated the data; KAR, TR and ODV analyzed the data and wrote the paper.

Competing Interests The authors declare no competing interests.

Materials & Correspondence Correspondence and requests for materials should be addressed to Orencio Durán Vinent (oduranvinent@tamu.edu).

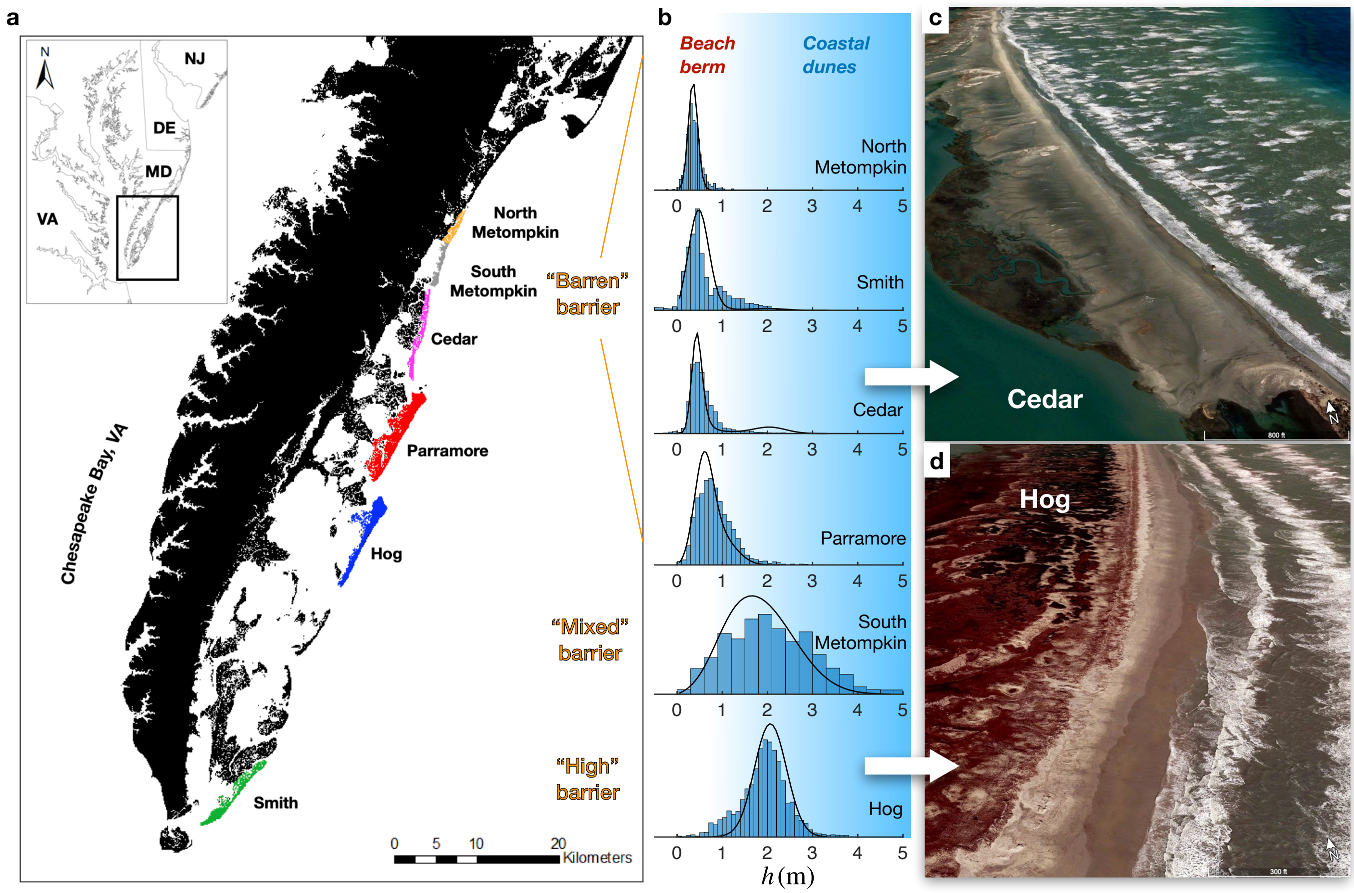

Figure 1: **Alongshore distribution of barrier elevation and barrier classification.** (**a**) The study area comprises the Virginia Barrier Islands (VBI), where we analyzed five representative islands and divided Metompkin into two sections (North and South) with very different morphological characteristics (Methods). (**b**) Alongshore distributions of barrier elevation h showing the three types of barrier islands classified based on their elevation: "Barren" islands ($h \lesssim$ 1m) that lack vegetated dunes and are dominated by a beach berm with typically unvegetated overwash fans (**c**), "high" islands ($h \gtrsim$ 1m) with well-developed dunes stabilized by vegetation (**d**), and "mixed" islands with a broad distribution of elevations (e.g. South Metompkin). The distribution functions predicted by our stochastic model (Eq. 2) are shown as solid lines in (**b**). Images from Google Earth.

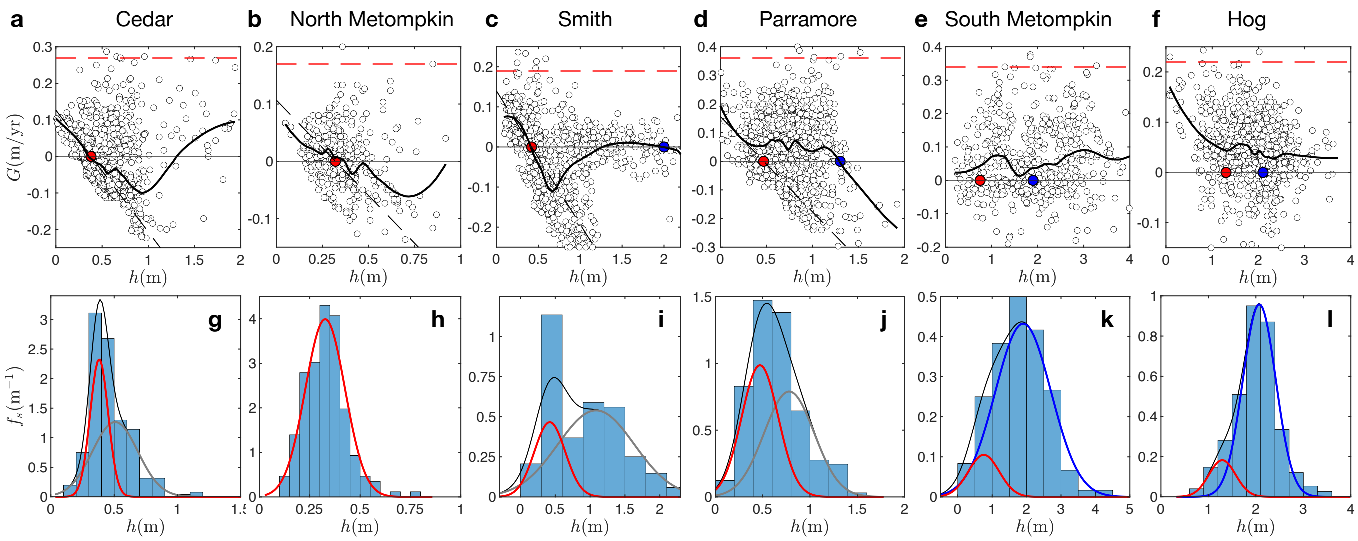

Figure 2: **Estimation of model parameters and stable equilibria in island dynamics.** (**a**–**f**) Rate of elevation change $G(y) = [h(y, 2017) - h(y, 2014)]/3\text{yr}$ for a given alongshore location y (dots) as function of the initial alongshore elevation $h(y, 2014)$ relative to the reference beach elevation (Methods). The solid line is the average growth rate $G(h)$. The red dashed line is the maximum dune growth rate G_d (Methods). (**g**–**l**) Probability density function f_s of elevations h with very small rates of change ($|G| < 2.5\text{cm/yr}$). Solid black line is a fit with two Gaussians, the first one (in red) describes the alongshore distribution $\mathcal{N}_{h_0}$ of the base elevation h_0. For Hog and South Metompkin (**k** and **l**), the second Gaussian (in blue) describes the alongshore distribution $\mathcal{N}_H$ of maximum dune elevations H (Methods). In (**g**–**j**), the Gaussian in gray has no clear interpretation. Red dots in (**a**–**f**) correspond to the lower-elevation stable equilibrium $\overline{h}_0$ defined by the mode of the red Gaussian in (**g**–**l**). In (**a**–**c**), this equilibrium is consistent with the formal definition $G = 0$ and $G' < 0$, as shown by the solid black line. The black dashed line in (**a**–**d**) shows the linear growth rate $G(h) = (\overline{h}_0 - h)/3\text{yr}$. Blue dots in (**c**–**f**) correspond to the dune stable equilibrium $\overline{H}$ defined either by the condition $G = 0$ and $G' < 0$ or by the mode of the blue Gaussian (**e**–**f**). See Methods for more details.

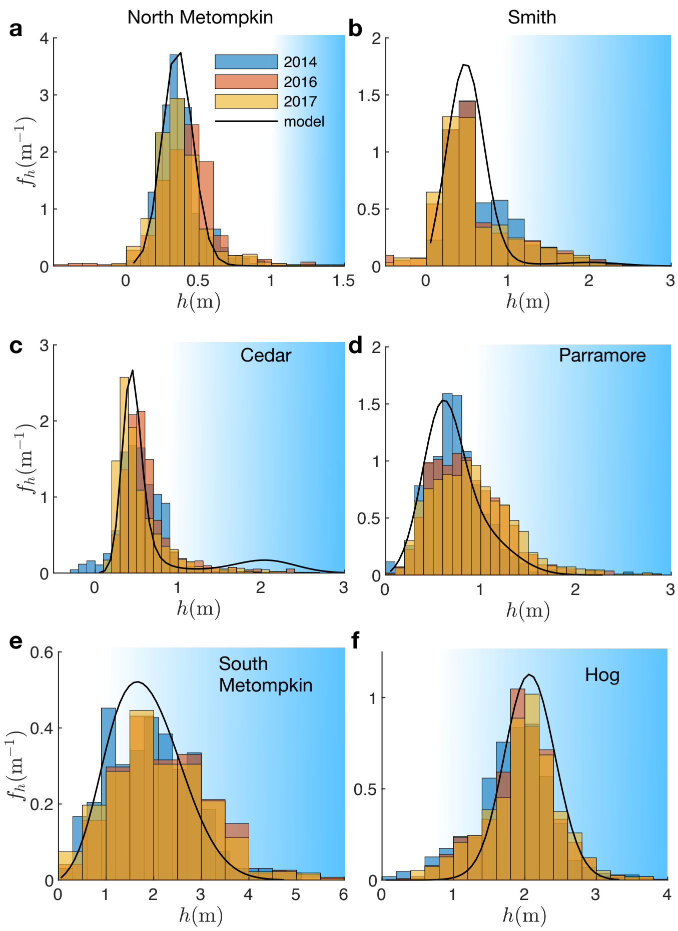

Figure 3: **Comparison with model predictions.** Probability distribution densities of dune heights (relative to the reference beach elevation, see Methods) obtained from real data for the three different years present in the analysis, and the predictions from the steady state stochastic model (solid lines). The model predicts the steady-state PDF from the parameters estimated for each island (Table 1).

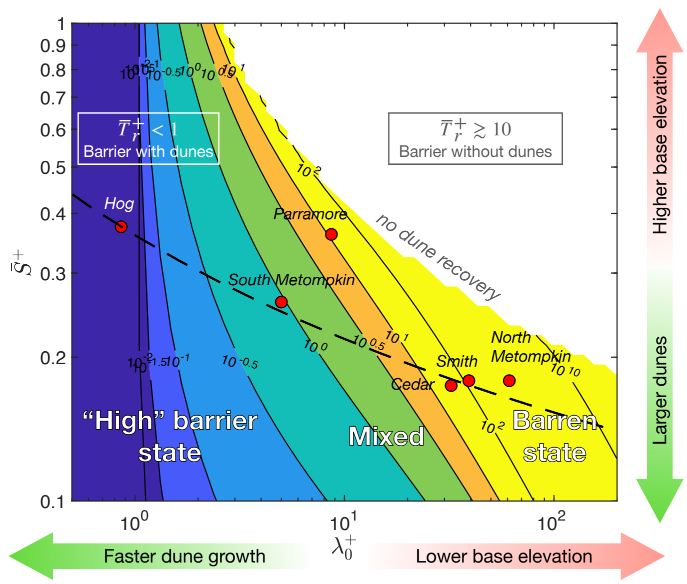

Figure 4: **Transition from 'high' to 'barren' barrier islands.** Barrier phase space showing the contour lines of the rescaled dune recovery time $\overline{T}_r^+$ (Methods) and the corresponding barrier classification as function of the two control parameters. Symbols representing the islands are based on the values in Table 1. The dashed line shows a parametric phase curve $(\lambda_0^+(\overline{h_0}), \overline{S}^+(\overline{h_0}))$ illustrating the transition from a 'high' barrier to a barren state as the base elevation $\overline{h}_0$ changes from 1.5m to 0 (left to right), while keeping all other parameters as for Hog island.

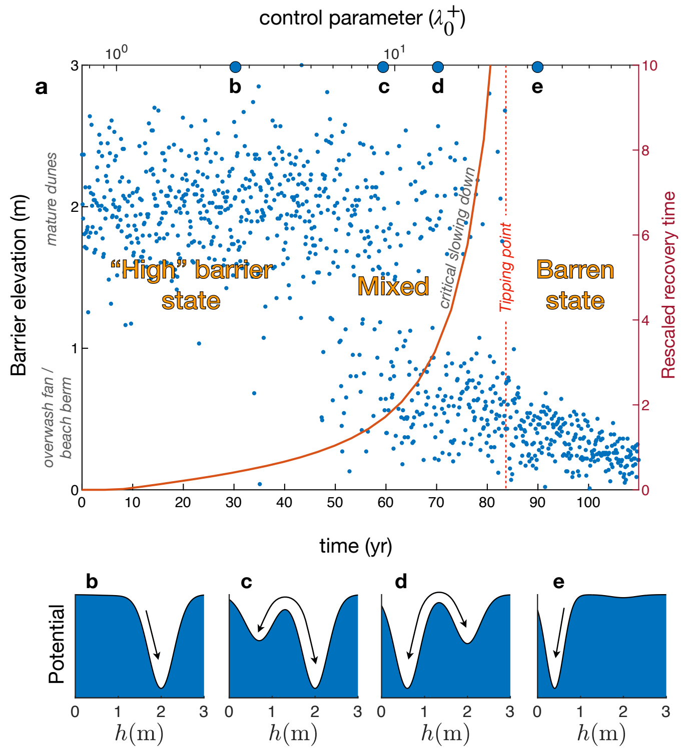

Figure 5: **Critical transition in barrier's elevation and the onset of potential barrier loss driven by SLR.** (**a**) Simulations of the steady-state stochastic dynamics, represented by the PDF $f_h(h|\lambda_0^+, \overline{S}^+)$ of barrier elevation h sampled four times per year (symbols), over the phase curve shown by the dashed line in Fig. 4. The parametric phase curve $(\lambda_0^+(\overline{h}_0), \overline{S}^+(\overline{h}_0))$ is function of mean base elevation $\overline{h}_0(t)$, which itself changes with time due to SLR as $\overline{h}_0(t) = 1.3\text{m} - Rt$. The rate R of relative SLR is assumed to be constant and equal to the average for the intermediate scenario estimated for the region from 2020-2050 ($R = 10\text{mm/yr}$) [43]. All other parameters are taken as for Hog island (Table 1). The rescaled dune recovery time $\overline{T}_r^+$ over the phase curve (solid line) shows the critical slowing down of the dynamics as it approaches the critical transition to the low-barrier state, represented qualitatively by a tipping point. (**b-e**) Approximate basin of attraction of the two most probable equilibirum elevations, the mean maximum dune height $\overline{H}$ and the mean base elevation $\overline{h}_0$, represented by the inverted PDF $f_h(h)$ and interpreted as a potential function [44].

Table 1: **Model parameters, control parameters and average island elevation for VBI.** Estimated model parameters: mean $\overline{h_0}$ (m) and rescaled standard deviation $\sigma_{h_0}/\overline{h_0}$ of the base elevation, mean $\overline{H}$ (m) and rescaled standard deviation $\sigma_H/\overline{H}$ of the maximum dune height, maximum dune growth rate G_d (m/yr), mean dune formation time in the absence of dune erosion $\overline{T_d}(yr) = (\overline{H} - \overline{h_0})/G_d$, mean frequency λ_r (yr^{-1}) and size $\overline{S}$ (m) of HWEs overtopping the reference beach elevation. Control parameters λ_0^+ and $\overline{S}^+$ (Eqs. 4 and 5). Measured and predicted mean island elevation (m), $\overline{h}_{\text{meas}}$ and $\overline{h}_{\text{pred}}$ respectively.

Island	$\overline{h_0}$	$\frac{\sigma_{h_0}}{\overline{h_0}}$	$\overline{H}$	$\frac{\sigma_H}{\overline{H}}$	G_d	$\overline{T}_d$	λ_r	$\overline{S}$	λ_0^+	$\overline{S}^+$	$\overline{h}_{\text{meas}}$	$\overline{h}_{\text{pred}}$
N. Met	0.32	0.32	2.1	0.17	0.17	10.5	18	0.3	61	0.18	0.39	0.35
Smith	0.42	0.52	2.1	0.17	0.19	8.8	18	0.3	39	0.18	0.61	0.55
Cedar	0.38	0.26	2.1	0.17	0.27	6.4	18	0.3	32	0.17	0.58	0.73
Parr.	0.47	0.42	1.3	0.22	0.36	2.3	18	0.3	8.7	0.36	0.84	0.71
S. Met	0.75	0.60	1.9	0.42	0.34	3.4	18	0.3	5.0	0.26	2.10	1.84
Hog	1.30	0.21	2.1	0.17	0.22	3.6	18	0.3	0.9	0.37	1.92	2.07